[27]P. Nozières, in *Polarization, Matiere et Rayonnement*, volume julibaire à l'honneur A. Kastler (Presses Universitaires de France, Paris, 1969).
[28]J. H. Van Vleck and V. F. Weisskopf, Rev. Mod. Phys. 17, 227 (1945).
[29]H. C. Torrey, Phys. Rev. 104, 563 (1956).
[30]T. Moriya, Progr. Theoret. Phys. (Kyoto) 28, 371 (1962); J. Phys. Soc. Japan 18, 516 (1963).
[31]S. Barnes (private communication).
[32]T. Sasada and H. Hasegawa (report of work prior to publication).
[33]B. Caroli, C. Caroli, and D. R. Fredkin, Phys. Rev. 178, 599 (1969).
[34]J. H. Pifer and R. T. Longo, Phys. Rev. B 4, 3797 (1971).
[35]S. Schultz (private communication).

PHYSICAL REVIEW B VOLUME 7, NUMBER 7 1 APRIL 1973

Properties of Simple Alkali-Tetracyanoquinodimethan Salts. I. Magnetic Behavior of Lithium Tetracyanoquinodimethan

Johan G. Vegter and Jan Kommandeur
Laboratory for Physical Chemistry, University of Groningen, Bloemsingel 10, Groningen, The Netherlands

Peter A. Fedders*
Department of Physics, Washington University, St. Louis, Missouri 63130
(Received 10 March 1972)

The absolute value of the spin susceptibility of the radical-ion salt Li^+TCNQ^- (tetracyanoquinodimethan) has been accurately measured in the temperature range of 100–450 °K. It is shown that the magnitude and temperature dependence of the susceptibility can be quantitatively explained on the basis of an elementary symmetry-split band theory for a linear system. The splitting is due to the "dimerization" along the chain of $TCNQ^-$ ions. The resulting values for bandwidths and band gap (0.055 and 0.135 eV, respectively) are in fair agreement with the values obtained from a tight-binding band-theory calculation on Rb^+TCNQ^-, for which the crystal structure is accurately known. The experimental results are also compared with other theoretical calculations. The results show band theory to be considerably superior in this particular case.

I. INTRODUCTION

After the appearance of the first paper concerning the electronic conduction and exchange interaction in tetracyanoquinodimethan (TCNQ) salts,[1] spin correlation in these complexes was intensively studied by a great number of investigators[2] and theoretical explanations for the correlation phenomena were suggested,[2] such as the single-triplet model,[3] the theory for the collective electronic states,[4] the Ising chain,[5] the linear Heisenberg antiferromagnet,[6] and the modified Hubbard model.[7] The absolute paramagnetic susceptibilities and electrical conductivities of the (1:1) (alkali)$^+$ $TCHQ^-$ salts, however, are not in agreement with these theories (see Sec. VI).

Recently, Fedders and Kommandeur[8] have shown that the temperature dependence of the spin susceptibilities of neutral organic-radical solids can be explained using a narrow-band model. It is the purpose of this paper to apply simple one-electron Bloch theory to the crystalline alkali TCNQ, which are pseudo-one-dimensional semiconductors.[9–11] Because of the large spatial extension of the TCNQ molecule and its large polarizability, the electron-electron Coulomb repulsion in TCNQ complexes is small compared to that in most inorganic salts. This is the reason for the success of the one-electron tight-binding model, even though the bandwidth is small (Sec. III).

One-dimensional band theory quantitatively accounts for the temperature-dependent paramagnetic-susceptibility behavior of LiTCNQ (Sec. IV), which indicates that the correlation energy can be neglected in this system. The optical and semiconductive properties are well understood on this basis and will be treated in a subsequent paper.

The application of band theory in the other alkali-TCNQ salts is hampered by the occurrence of phase transitions.[12] However, the susceptibilities of the high-temperature phases can easily be understood in terms of this model, while a consideration of the total free energy of electrons and lattice[13] readily gives insight into the properties of the low-temperature phase.

II. EXPERIMENTAL

A. Preparation of M^+TCNQ^- Salts

TCNQ was prepared as described by Acker and Hertler[14]; before use, it was sublimed *in vacuo*. Li^+TCNQ^- was prepared by the well-known prescription of Melby *et al.*[15] from solutions of lithium iodide and TCNQ in acetonitrile. Crystalline ma-

terial could be obtained by carrying out the preparation at room temperature, using the crystal-growth apparatus described by Pott and Kommandeur.[16] In this diffusion technique, spectrograde acetonitrile, distilled and dried over P_2O_5, was used as a solvent. The acquisition of crystalline LiTCNQ was very sensitive to the concentrations of the starting solutions. Best results were obtained by starting with a 0.046-molar LiI solution and a 0.016-molar solution of TCNQ in acetonitrile. In this way small polycrystalline bits could be collected in 12 h. The same procedure was used in preparing crystals of the other M^+TCNQ^- salts. With this technique we obtained polycrystalline NaTCNQ and needles of K-, NH_4-, and Rb-TCNQ. CsTCNQ needles, sometimes contaminated with the (2 : 3) compound, were prepared from metathesis of CsCl with an aqueous solution of LiTCNQ, followed by recrystallization from acetonitrile.

B. Measurements

Absolute spin-susceptibility measurements were performed with a modified Varian V-4500 EPR X-band spectrometer and associated 12-in. electromagnet. Replacement of the detection by an integrating circuit, which allows digital registration of the paramagnetic intensity without the need for a diamagnetic correction, yields an accuracy of about 0.5–3%.[17] The apparatus was calibrated with a few freshly prepared weighed single crystals of Wurster's blue perchlorate. It is assumed that the paramagnetic susceptibility of these crystals ideally fits a Curie–Weiss law for spins of $\frac{1}{2}$ with a g factor of 2.003[18]:

$$\chi = C(T - \Theta)^{-1}.$$

Θ was independently determined by means of the integration technique and amounts to -33.9 °K. The Curie constant per mole pure substance was $C = 0.3763$ emu °K. Static-susceptibility measurements[19] on Wurster's-blue-perchlorate crystals showed $99 \pm 2\%$ "free radical," agreeing with the above assumption. Temperature-dependent measurements were performed with a variable-temperature device (100–550 °K). Care was taken with the microwave power so as to prevent any saturation effects of the ESR resonance signal, which are especially important at low temperatures.

The electronic absorption spectra were measured in the range between 4000–44000 cm^{-1} and were recorded with a Cary spectrophotometer Model No. 14. Spectra were taken of transparent films of solid M^+TCNQ^- salts, prepared by either of the following methods. (a) The reasonable solubility of LiTCNQ in acetonitrile, acetone, etc., permitted the preparation of LiTCNQ films by evaporation on a small quartz plate of its solution in these solvents. (b) The other alkali salts are sparingly soluble, so method (a) cannot be applied. However, films can be prepared by rubbing out the solid material on a polished plate of quartz.

Spectra of LiTCNQ films, prepared by both methods, hardly differ, except for a small blue shift of the low-energy band when method (b) is used. Besides this, the reliability of this method was checked by taking crystalline spectra of TCNQ and anthracene, which agreed very well with the known spectra of these materials.

III. THEORY

A. Justification of the Model

It is well known[20] that correlation effects usually prevent the straightforward application of one-electron band theory to electrons in a lattice in the limit of small transfer integrals between the constituents of the lattice. In particular, when the energy U of the doubly occupied (or "ionized") states in the Wannier representation exceeds this interaction the simple one-electron band theory is expected to fail. In the chainlike TCNQ-ion lattice, however, it may well be that the "ionized" states are not so high in energy.[21] This is due to the rather peculiar geometry of the TCNQ molecule. SCMO-CI (self-consistent molecular orbital with configuration interaction) calculations of Lowitz[22] and Jonkman and Kommandeur[23] have shown that in $TCNQ^-$ and $TCNQ^{--}$ the charges are located mainly on the $C(CN)_2$ "tails" (see Fig. 1) and to a high degree of approximation the charge distribution in a TCNQ-ion pair can be given as in Fig. 2(a). For the "gasphase"-disproportionation reaction [cf., Fig. 2(b)]

$$TCNQ^- + TCNQ^- \rightarrow TCNQ^0 + TCNQ^{--},$$

Jonkman and Kommandeur[23] calculated an energy increase of 3.5 eV. In the solid, however, the repulsion of the neighboring $TCNQ^-$ ions should be subtracted. A partial-charges calculation based on the charge distributions in $TCNQ^0$, $TCNQ^-$, and $TCNQ^{--}$[23] gives, for the usual TCNQ–TCNQ distance of 3.3 Å, a value of 2.8 eV, which should be subtracted from the disproportionation energy, leaving about 0.7 eV. Polarization further decreases this energy.

The gain in polarization energy for a doubly ionized state is equal to the polarization caused by an electric dipole in a neutral molecular lattice along with the monopole polarization of each of the constituents of this dipole caused by its charged partner. The latter contribution is about $\alpha e^2/R^4$, where e is the electronic charge, R is the nearest-neighbor distance, and α is the polarizability of the TCNQ molecule (ion). Various estimates

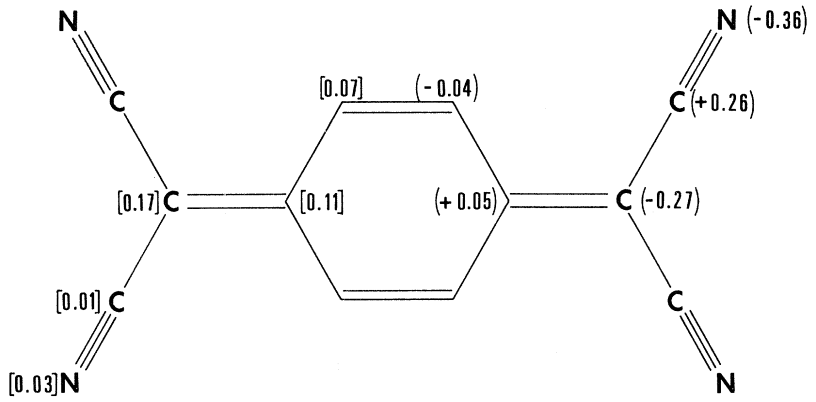

FIG. 1. Charge distribution ( ) and spin distribution [ ] in the $TCNQ^-$ ion (Ref. 23).

have been made for a molecular crystal; a value of about 1.0 eV does not appear at all unreasonable.[24]

In summary, we come to the conclusion that the disproportionation energy, i.e., the energy to form a doubly ionized state may be small if not zero for a TCNQ-neighboring pair. [It is tempting to extend these calculations to molecules with similar configurations such as tetramethyl-*p*-phenylenediamine (TMPD),[25] and maybe even diphenylpicrylhydrazyl (DPPH),[8] but we will here confine ourselves to TCNQ.] For non-neighboring pairs, the disproportionation energy will be higher, but polarization and interaction between pairs should also be taken into account and therefore, at finite excitation densities, these long-range pairs are perhaps not at such a high energy either. In any case, the stationary states of the crystal would be given by a complete configuration-interaction calculation of all possible charge configurations, which would be a formidable task.

Application of band theory requires that all doubly ionized Wannier states lie within the bandwidth. This may not strictly be the case, but if a sufficiently large fraction does, band theory can still be applied. In Sec. III B we will describe the band theory for the present case and then show, that it gives good results for the radical-ion salts considered.

B. Band Model

One-dimensional band theory will now be applied to the alternating linear ion-radical system, present in the crystalline M^+TCNQ^- salts. The unpaired electrons are tightly bound to the molecular cores and the overlap of the electronic wave functions on neighboring lattice sites will be small. As proposed by Fedders and Kommandeur, a tight-binding approximation (linear combination of molecular orbitals) will be used in calculating the electron states of the lattice.

From a variational calculation together with the Bloch theorem applied to a linear chain consisting of $\frac{1}{2}N$ unit cells, each containing two molecules, an expression for the energies of the one-particle states in the ground-state split-band system is derived in the Appendix,

$$E(k) = \pm (h_1^2 + h_2^2 + 2h_1 h_2 \cos ak)^{1/2} , \tag{3.1}$$

where h_1 and h_2 are transfer integrals between a molecule and its two inequivalent neighbors,

$$h_{1,2} = \int \varphi_{1,2}^* V' \varphi_0 \, dx . \tag{3.2}$$

V' is the lattice potential deriving from all sites except the site labeled zero. The φ's are π-electron wave functions for the unpaired electrons on neighboring molecules. The squares of these h integrals denote the tunneling probability of an electron from one ion to its neighbors on either side.

In (3.1) a is the unit-cell length and $k = 4n\pi/Na$, where n runs from $-\frac{1}{4}N$ to $+\frac{1}{4}N$. Each of both bands consists of $\frac{1}{2}N$ states. Assuming $|h_2|$ to be the smaller of the absolute values of both transfer integrals, the width E_b of each band is given by

$$E_b = 2|h_2| \tag{3.3}$$

and the separation between these bands is $2E_g$, where

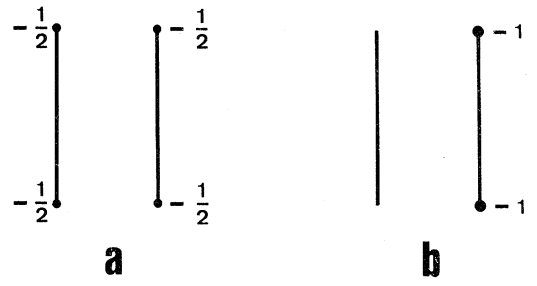

FIG. 2. Approximate charge distribution in (a) pair of $TCNQ^-$ ions, (b) disproportionated pair.

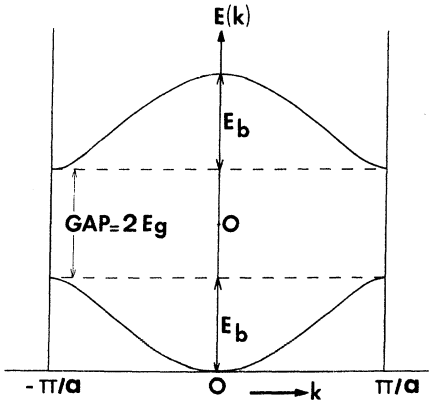

FIG. 3. Split-band system derived for an alternating linear chain.

$$E_g = |h_1| - |h_2| . \tag{3.4}$$

The total width, from the bottom of the lower band to the top of the higher band is E_w,

$$E_w = 2(E_b + E_g) = 2|h_1| + 2|h_2| . \tag{3.5}$$

It is more convenient, for this particular one-dimensional model, to parametrize the band system slightly differently. Instead of Eq. (3.1), we write

$$E(k) = \pm E_c(g^2 + \cos^2 \tfrac{1}{2}ak)^{1/2} , \tag{3.6}$$

with

$$E_c = 2(h_1 h_2)^{1/2} \tag{3.7}$$

and

$$g = \frac{E_g}{E_c} = \sinh\left(\frac{1}{2}\ln\left|\frac{h_1}{h_2}\right|\right) . \tag{3.8}$$

[If h_1 and h_2 possess opposite signs then $E_c = 2(|h_1 h_2|)^{1/2}$ and in the $E(k)$ expression $\cos^2 \frac{1}{2}ak$ is replaced by $\sin^2 \frac{1}{2}ak$, which only means a shift of π/a in the one-dimensional k space.] We obtain the usual band system as depicted in Fig. 3.

C. Calculation of the Susceptibility

In order to calculate the spin susceptibility quantitatively on the basis of this band model, we write down the grand partition function in the presence of a magnetic field H for this Fermi–Dirac system,[8,26]

$$Z = \sum_{(k,\sigma_k)} \sum_{n(k,\sigma_k)} \exp\{[-\beta E(k, \sigma_k) - \alpha] n(k, \sigma_k)\} , \tag{3.9}$$

where $n(k, \sigma_k)$ is the occupation number of the state (k, σ_k) and $\beta = 1/kT$; the second summation is over all sets $n(k, \sigma_k)$ with each member of the set taking on the values 0 or 1.

The energy of the one-particle state (k, σ_k) now reads

$$E(k, \sigma_k) = E(k) + \tfrac{1}{2}\sigma_k g \mu_B H . \tag{3.10}$$

$\sigma_k = +1, -1$ stands for spin-down and spin-up electrons, respectively. The dimensionless quantity α in (3.9) is related to the Fermi energy E_F,

$$\alpha = -\beta E_F \tag{3.11}$$

and is determined by the number of electrons (N_e) in the crystal,

$$N_e = -\frac{\partial \ln Z}{\partial \alpha} , \tag{3.12}$$

which is not necessarily equal to the number of lattice sites N. There may be a small excess or deficit of electrons due to lattice imperfections, such as nonstoichiometry, for instance. This deviation is governed by the parameter δn, defined by the relation

$$N_e/N = 1 + \delta n . \tag{3.13}$$

The zero-field spin susceptibility can be derived from the grand partition function via the relation

$$\chi = \lim_{H\to 0} \chi(H) = \lim_{H\to 0}\left(\frac{1}{\beta H}\frac{\partial \ln Z}{\partial H}\right) . \tag{3.14}$$

The expression (3.9) for Z can be rewritten in the completely factored form

$$Z = \prod_{k,\sigma} \{1 + \exp[-\beta E(k, \sigma_k) - \alpha]\} . \tag{3.15}$$

This equation enables us, together with (3.12) and (3.13), to write down an implicit expression for α terms of the density of states given by (3.6) and δn, summations having been replaced by integrations:

$$\begin{aligned}\delta n = \frac{1}{\pi}&\int_{-1/2\pi}^{1/2\pi} (e^{\alpha - \beta|E(k)|} + 1)^{-1} d(\tfrac{1}{2}ak) \\ &- \frac{1}{\pi}\int_{-1/2\pi}^{1/2\pi} (e^{-\alpha - \beta|E(k)|} + 1)^{-1} d(\tfrac{1}{2}ak) \\ &= -\frac{1}{\pi}\int_{-1/2\pi}^{1/2\pi}\left(\frac{\sinh\alpha}{\cosh\alpha + \cosh\beta E(k)}\right) d(\tfrac{1}{2}ak) .\end{aligned} \tag{3.16}$$

In the same way we arrive from (3.14) and (3.15) at a parametric expression for the spin susceptibility,

$$\begin{aligned}\frac{\chi T}{C} = \frac{1}{\pi}&\int_{-1/2\pi}^{1/2\pi} e^{\alpha + \beta|E(k)|}(e^{\alpha + \beta|E(k)|} + 1)^{-2} d(\tfrac{1}{2}ak) \\ &+ \frac{1}{\pi}\int_{-1/2\pi}^{+1/2\pi} e^{\alpha - \beta|E(k)|}(e^{\alpha - \beta|E(k)|} + 1)^{2} d(\tfrac{1}{2}ak),\end{aligned} \tag{3.17}$$

where C is the Curie constant.

Numerical results were obtained by solving (3.16) for α, using a self-consistent method for fixed values of δn, g, and βE_c, with the aid of a

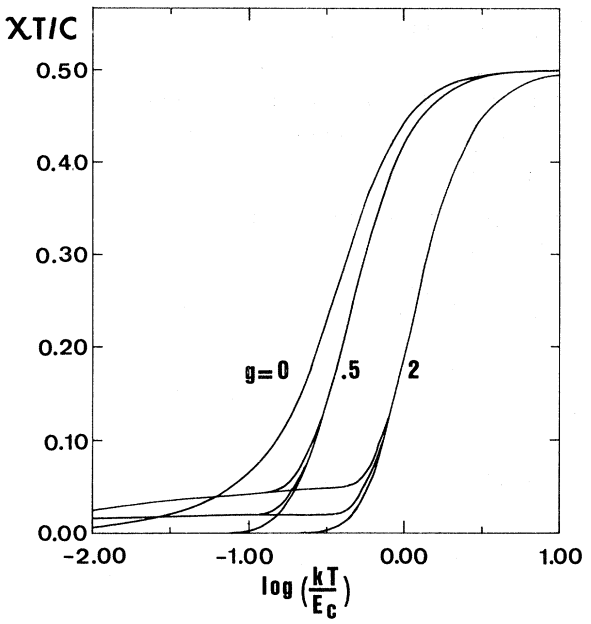

FIG. 4. Computer-calculated curves of $\chi T/C$ vs log (kT/E_c) for different values of the parameters g and δn; $g=0$, 0.5, and 2 from left to right, whereas $\delta n=0.05$, 0.02, and 0 from top to bottom in the low-temperature region.

Telefunken TR4 computer.

It is most convenient to compute α and $\chi T/C$ subsequently from (3.17), as a function of βE_c with constant parameters δn and g. Generalized plots of $\chi T/C$ vs the reduced temperature kT/E_c can be obtained now as shown in Fig. 4 for various values of g and δn. At very low temperatures the absolute values of δn determine the susceptibility. In the split-band system, a small excess of electrons, for instance, will remain in the upper band even at 0 °K. They give rise to a temperature-independent Pauli susceptibility, whereas at somewhat higher temperatures they behave in a Curie fashion. If the temperature increases further, the excitation of electrons across the gap will soon become dominant and a sharp rise in the susceptibility results. At high temperatures ($kT > E_w$) all curves bend towards $\chi T/C=0.50$, the limit for the unperturbed band system.[8] Experimental-susceptibility data, transformed into a $\chi T/C$-vs-$\log_{10}T$ plot, enable us to uniquely determine the relevant band parameters by comparison with the computed curves of Fig. 4. If these curves are plotted on the same scale, then the horizontal shift, needed for coincidence of the experimental and one of the calculated curves, yields E_c; the slope of the coinciding curves then determines the g value. δn is easily found from the almost-flat low-temperature portion. The band gap $2E_g$ then follows from (3.8), whereas the width of each band can be calculated from (3.6),

$$E_b = E_c(g^2+1)^{1/2} - E_c g. \tag{3.18}$$

In Sec. IV the experimental-susceptibility data for LiTCNQ will be explained quantitatively on the basis of this band model.

Finally, a remark should be made on the nature of δn. As stated earlier in this section it may arise from nonstoichiometry. In this case an incidental replacement of a $TCNQ^-$ in the linear chain by $TCNQ^{--}$ or $TCNQ^0$ accounts very well for an excess or deficit of electrons, respectively. However, the occurrence of an "impurity contribution" at low temperatures in the paramagnetic susceptibility may also be due to a small extend of disorder in the crystalline material. The theory of amorphous semiconductors[27] shows the existence of tails of localized states at the various band edges. So the effect of an impurity content may equally well be ascribed to a fraction of localized single-particle states in both hands. Electrons accommodated in these states will exhibit a Curie-type susceptibility at (very) low temperatures and not a Pauli susceptibility.

IV. RESULTS

Polycrystalline LiTCNQ exhibits a single electron-spin-resonance (ESR) absorption line down to 77 °K; the linewidth is about 1.5 G. From this ESR signal the absolute spin susceptibilities were determined by the integration technique mentioned in Sec. II. The experimental values of $\chi T/C$ vs temperature for crystalline LiTCNQ, obtained from two independent measurements, are shown in Fig. 5. At room temperature the susceptibility is 6.1% of the Curie susceptibility χ_c; it rapidly falls off with decreasing temperature and below 150 °K it practically behaves in a Curie fashion with $\chi=0.031\chi_c$, where $\chi_c=C/T$.

This curve enables us to determine the band parameters E_c and g as described in Sec. III; the results are $E_c/k=1185$ °K and $g=0.66$. From these we derive a bandwidth $E_b/k=640$ °K and half of a band gap of $E_g/k=780$ °K; the excess or deficit of electrons amounts to 3.4% as determined from the flat portion of the curve. The excellent agreement between theory and experiment is demonstrated by the calculated curve of $\chi T/C$ vs temperature, which completely coincides with the drawn experimental curve. This agreement is also shown in the susceptibility versus temperature curve for LiTCNQ, which looks somewhat peculiar at first sight. In Fig. 6, the drawn line gives a result of a calculation with the parameters mentioned and again compares theory with experiment. It is important to note that a temperature-dependent spin-susceptibility measurement on another crystalline LiTCNQ sample could equally well be

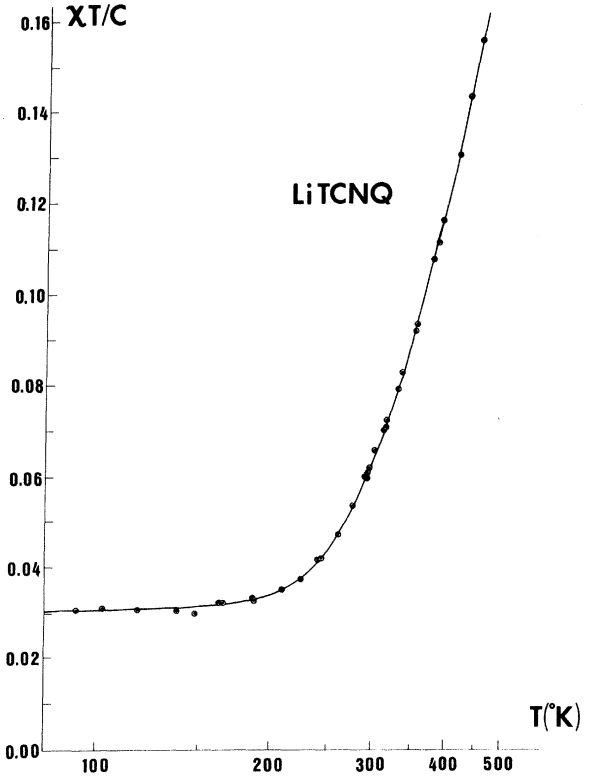

FIG. 5. Comparison of experimental and theoretical values of $\chi T/C$ for LiTCNQ; $E_g/k = 780\,^\circ\mathrm{K}$, $E_b/k = 640\,^\circ\mathrm{K}$, and $\delta n = 0.034$.

described with the same band parameters E_c and g; δn, however, appeared to be somewhat different (0.031), showing the variable nature of this parameter for a given substance, as would be expected (Fig. 6). Although theory predicts a Pauli-type susceptibility for an excess or deficit of electrons in the band system at very low temperatures, it will be very difficult to investigate this experimentally. Extension of the calculations, with the parameters found for LiTCNQ to low temperatures indicates that this temperature-independent portion of the susceptibility eventually appears at temperatures below 1.3 °K. Similar measurements on CuTCNQ have been reported in a previous paper.[13] These results can be interpreted in the same way as for LiTCNQ but with a much lower impurity content ($\delta n = 0.05\%$).

V. DISCUSSION

The impossibility of obtaining sufficiently large LiTCNQ single crystals has so far prevented an exact crystal-structure determination. Fortunately, the structure of the low-temperature phase of RbTCNQ was investigated recently by Hoekstra, Spoelder, and Vos[10] and in order to check the above results for LiTCNQ, we performed some calculations with reference to this RbTCNQ structure, assuming this structure also to be basic to the other simple alkali TCNQ.

Crystalline RbTCNQ has monoclinic symmetry and belongs to the space group $P2_1/c$.[10] Figure 7 shows the essential part of this structure, which consists of fairly isolated rows of $TCNQ^-$ ions along the a axis, surrounded by Rb^+. Similar rows have also been observed in a number of other TCNQ complexes[11,28,29] and in TCNQ itself.[30] The figure shows the stacking of the $TCNQ^-$'s within such a row; the ions have the shape of a shallow boat, because the quinoid rings bend towards one another, so as to give the appearance of dimers. Some spacings of interest are given in the figure. It is important to note that theoretical calculations for the $TCNQ^-$ ion reveal that the greater part of the *spin density* (i.e., the electron density in the "valence orbital") is carried by the flat quinoid skeleton, whereas the total electronic charge is almost entirely located on both $C(CN)_2$ "tails" (cf. Fig. 1).[22,23]

The dimerlike behavior of the $TCNQ^-$'s, within a row, also appears in the electronic absorption spectrum of the solid M^+TCNQ^- salts, as given in Fig. 8 for RbTCNQ. Peaks arise at about 38 600, 27 300, 16 100, 11 800, 10 400, and 7600 cm^{-1}. This spectrum turns out to be almost independent of the counter cation M^+(M = Li, Na, K, NH_4, Rb, Cs) except for the location of the low-energy band and the observability of the 11 800- and 10 400-cm^{-1} absorptions. These crystalline electronic spectra strongly resemble those observed by means of a diffuse-reflectance technique at room temperature by Iida.[31] Moreover, these spectra are similar to that of the $(TCNQ)_2^{2-}$ dimer observed by Boyd and Phillips in a concentrated aqueous solution of LiTCNQ,[32] with absorption peaks at 27 000 and 15 600 cm^{-1}. This spectroscopic evidence supports "dimerization" at least of the "valence orbitals" of the ion radicals in the solid state. A further plausibility of this statement can be found in the crystalline spectrum of (N-methylphenazinium)$^+$ $TCNQ^-$.

According to Fritchie,[28] the $TCNQ^-$ ions in this compound form a regular chain with a relatively small interplanar distance of 3.26 Å. Probably because of the lack of alternation in these $TCNQ^-$ chains, the crystalline spectrum[31] is much less similar to the dimer spectrum than in the M^+TCNQ^- salts, just discussed. The band at 11 800 cm^{-1} is much more pronounced and the dimer band at 16 400 cm^{-1} is strongly suppressed in the phenazinium complex.

Although the foregoing comparisons of spectra are useful, they do not give an explanation of the observed crystalline spectra of the M^+TCNQ^- salts. In a subsequent paper we will show the

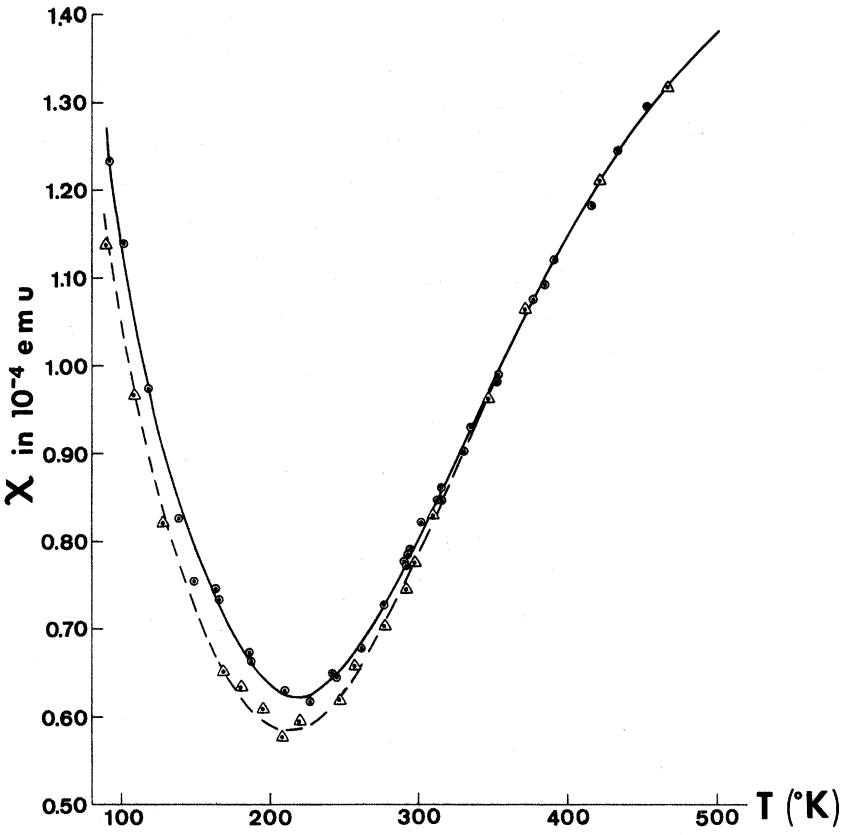

FIG. 6. Temperature dependence of the molar spin susceptibility of LiTCNQ. Drawn line is calculated curve with parameters $E_c/k = 1185\,^\circ\mathrm{K}$, $g = 0.66$, and $\delta n = 3.4\%$; line is calculated curve with the same E_c and g, $\delta n = 3.1\%$; ⊙, experimental points of crystal I; △, experimental points of crystal II.

ability of band theory to explain these spectra at least in a qualitative way.

The spectral resemblance of all (alkali)$^+$TCNQ$^-$ salts involved and their striking similarity with the dimer spectrum lend more credence to our assumption that the RbTCNQ structure is also basic to the other alkali TCNQ. Furthermore, this structure justifies our theoretical discussion of these systems as linear chains with alternating interionic distances.

As discussed in the Appendix the band parameters E_c and g (or E_g and E_b) in the tight-binding approximation are mainly determined by the transfer integrals h_1 and h_2 between neighboring molecules. A numerical estimate of these integrals can be obtained by substituting a simple Coulombic interaction potential e^2/r for the potential-energy expression in Eq. (3.2). The π-electron wave function for the unpaired electron on the radical ions was written as a linear combination of atomic-Slater-type $2p\sigma$ functions with an effective nuclear charge of 3.4; the coefficients were taken from Jonkman and Kommandeur's results, who compared SCMO CI calculations in the Pariser–Parr–Pople (PPP) approximation for TCNQ, TCNQ$^-$, and TCNQ^{--} with one fairly reliable set of parameters.[23] In this approximation both h integrals were calculated for the known atomic positions in RbTCNQ[33] and Table I shows their relation to the mutually dependent pairs of band parameters (E_c, g) and (E_b, E_g). The agreement between the experimental and theoretical band parameters is reasonable, probably validating *a posteriori* some of the assumptions that have been made. It should, moreover, be realized that wave functions have been used that are "calibrated" on energy, optical transitions, and spin densities, properties sensitive to the internal structure of the TCNQ$^-$ ion. The band parameters derive from the external part of the wave function, about which very little is known.

Applying band theory, it is also very interesting

TABLE I. Comparison of experimental LiTCNQ and calculated RbTCNQ parameters.

	LiTCNQ (experimental)	RbTCNQ (calculated)
$g = \sinh(\frac{1}{2}\ln\lvert h_1/h_2\rvert)$	0.66	0.67
$E_c = 2(\lvert h_1 h_2\rvert)^{1/2}$	1185 °K	2010 °K
$E_b = 2\lvert h_2\rvert$	640 °K	1075 °K
$E_g = \lvert h_1\rvert - \lvert h_2\rvert$	780 °K	1340 °K
$E_w = 2\lvert h_1\rvert + 2\lvert h_2\rvert$	2840 °K	4830 °K

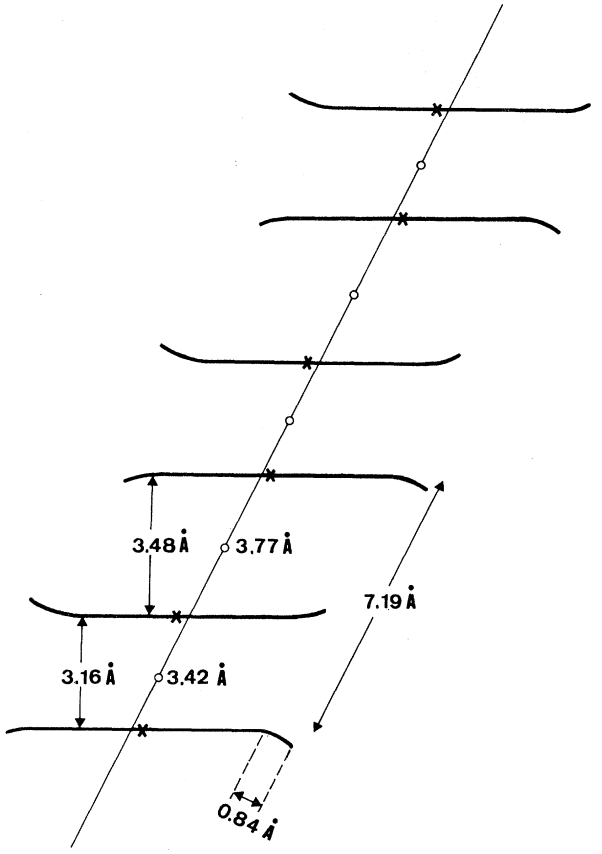

FIG. 7. Stacking of the $TCNQ^-$ ions in a chain (RbTCNQ) (Ref. 10).

to consider complex salts like $M^+(TCNQ)_2^-$; here the number of electrons is half the number of lattice sites and now even the lower band is half-filled and the system will tend to split once more (Fig. 9). At low temperatures all electrons can again be found in the lowest band and a small excess will again give rise to a Curie-type "impurity" behavior. If at higher temperatures the small gap is no longer felt by the electrons, the material will act like a metal, as shown by its high conductivity and the Pauli susceptibility. These properties have been observed by Kepler in the quinolinium salt with $\chi_P \approx 5.0\times10^{-4}$ emu.[34] From his measurements, one derives a total width of the band system of about 3000–4000 °K for this complex, which is again of the same order of magnitude as found for E_w (2840 °K) in LiTCNQ.

Another interesting quantity that can be calculated from the LiTCNQ band structure is the effective number of charge carriers,[35]

$$N_{eff} = \frac{Na}{2\pi}\int \frac{m_e}{m_k^*} f_k^0 dk \qquad (5.1)$$

integrated over both hands. In this equation, N is the number of ion radicals per cm^3 (3.5×10^{21}); m_e and m^* are the free and effective electron mass, respectively, where $m_k^* = \hbar^2[d^2E(k)/dk^2]^{-1}$ can be deduced from Eq. (3.6) and f_k^0 is the Fermi–Dirac distribution function $1/\{\exp[\beta E(k)+\alpha]+1\}$. Substituting the band parameters found for LiTCNQ, one calculates $N_{eff} = 2.2\times10^{19}/cm^2$ at 300 °K; a very reasonable number in view of experimental data available from Hall-effect measurements on (triethylammonium)$^+$ $(TCNQ)_2^-$. In this complex Farges *et al.*[36] derive an N_{eff} of about 3×10^{19} cm^3 at room temperature. As the number of free spins in LiTCNQ at 300 °K is $N\chi T/C = 2.2\times10^{20}/cm^3$, the charge carriers in both bands possess an average effective mass $\langle m_k^*\rangle = 10m_e$. At the band edges ($k = \pm\pi/a$), we derive $|m_k^*| = 4\hbar^2 g/a^2 E_c \approx 4m_e$.

Finally, we compare bandwidth and band gap in LiTCNQ with those found in neutral organic-radical systems.[8] The magnetic susceptibilities of DPPH are well explained with a bandwidth and band gap of the order of a few degrees Kelvin. The planar carbazyl group in the structurally related picrylamino-carbazyl (PAC) will allow for a larger overlap between neighboring molecules and higher values for the band parameters are expected, in agreement with the experimentally derived bandwidth $E_b/k = 105$ °K and band gap $2E_g/k = 180$ °K.

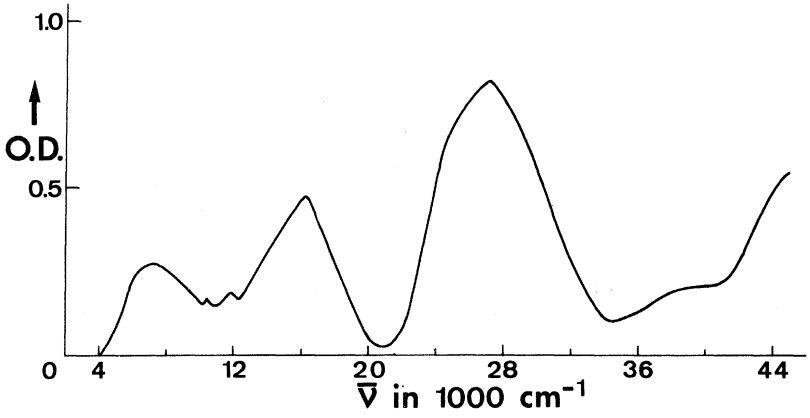

FIG. 8. Electronic absorption spectrum of solid RbTCNQ.

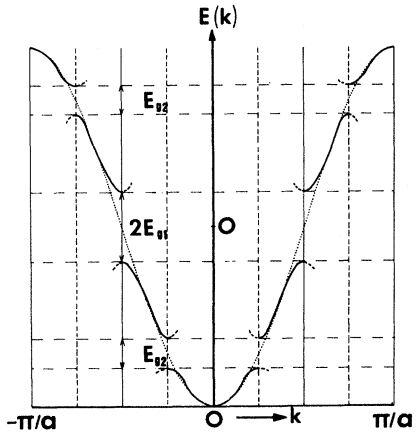

FIG. 9. Doubly split-band system in $M^+(TCNQ)_2^-$.

The still higher values in LiTCNQ can be explained as a consequence of the partial localization of the greater part (85%[23]) of the *spin density* on the quinoid skeleton. Figure 7 illustrates the arrangement of $TCNQ^-$ ions in RbTCNQ, which is such as to allow an appreciable π overlap between regions of highest spin density on nearest neighbors, while retaining almost equal separation between the charge carrying "tails." Moreover, the distance 3.16 Å between suscessive $TCNQ^-$'s is one of the shortest interplanar TCNQ spacings observed so far. Assuming a similar structure for LiTCNQ, these arguments account well for the relatively large total width of the band system in this material.

VI. COMPARISON WITH OTHER THEORIES

In this section, the experimental-susceptibility data for LiTCNQ and their theoretical interpretation as given in this paper, will be compared with those predicted by theories presented up to now, such as (a) the simple singlet-triplet theory for dimers in the valence-bond (VB) approximation,[37] (b) the molecular-orbital (MO) treatment of isolated dimers, (c) the linear Ising model,[5] and (d) the alternating linear-Heisenberg-antiferromagnetic chain.[6,38]

(a) The well-known expression for singlet-ground-state dimers, each having a triplet state lying at an energy ΔE above this ground state is in the case of noninteracting triplets

$$\chi T/C = \tfrac{4}{3}\,(1+\tfrac{1}{3}e^{\Delta E/kT})^{-1}. \qquad (6.1)$$

Conventionally, ΔE is estimated from the slope of curve I given in Fig. 10; this curve is obtained from the experimental data (Fig. 5) after subtraction of the low-temperature Curie part, which is usually put down to impurities. A straight line is only obtained in the high-temperature region, which is not in accordance with (6.1). A more accurate ΔE value is obtained from the drop off of the *relative* ESR intensity (I) with temperature, using

$$I(T) \sim (1+\tfrac{1}{3}e^{\Delta E/kT})^{-1}. \qquad (6.2)$$

The best fit is acquired with $\Delta E/k = 1200$ °K (0.103 eV). However, this ΔE value substituted in (6.1) yields an absolute susceptibility far higher than experiment (see curve I of Fig. 11). The deviations amount to 60–70% above room temperature. The exponential behavior of $I(T)$ vs $1/T$ is often ascribed to a system of noninteracting triplets. An accurate inspection of the *absolute* spin susceptibilities will generally contradict this assumption in these solids. Naturally, (6.1) can be fitted by assuming ΔE to be temperature dependent; the result for LiTCNQ is an increasing ΔE value with increasing temperature ($\Delta E = \Delta E^0 + 0.7kT$, amounting to an increase in ΔE of 15% over the temperature region of interest), contrary to predictions from theoretical viewpoints[2,6,38] and observations in other TCNQ complexes.[34,39]

(b) The above VB treatment of pure dimers characterizes the limiting case in which the contribution of doubly occupied states is neglected. As is well known, in the MO treatment, one possibly overestimates the occurrence of these "ionized" states by giving them equal weight as the states of single occupancy, neglecting the intrasite electron-electron interaction. For comparison the MO calculation of the dimer, given below, may be of interest.

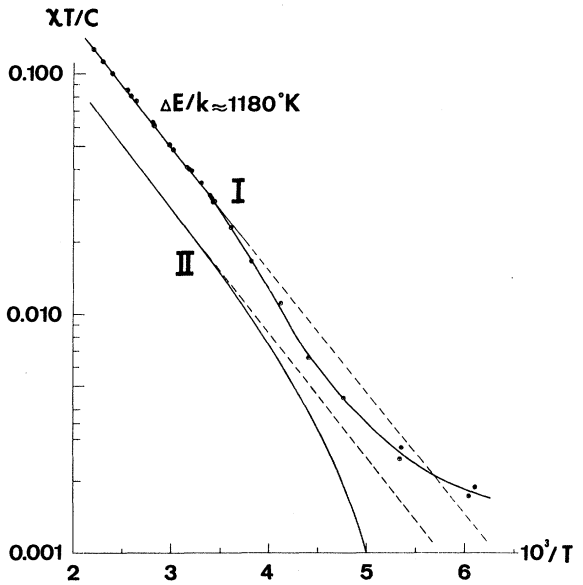

FIG. 10. Curve I: behavior of $\chi T/C$ vs $1/T$ for the LiTCNQ susceptibility data, after subtraction of the "impurity" contribution (3.06%). Curve II: comparison with the modified Ising model (Ref. 5).

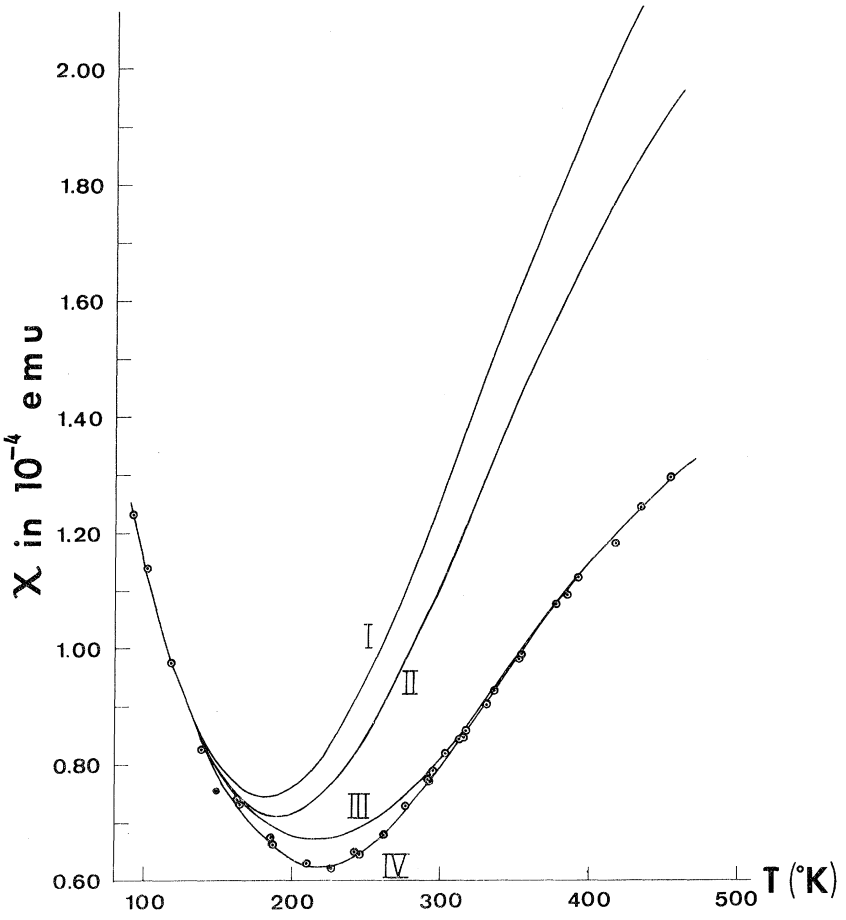

FIG. 11. Comparison of various theories with experiment: I, singlet-triple theory (VB) for dimers, (Ref. 27); II, MO treatment of isolated dimers; III, alternating linear-Heisenberg-antiferromagnetic theory (Ref. 6); IV, split-band theory (present study). A Curie-type impurity (3.06%) contribution has been added to curves I, II, and III.

The MO scheme for an isolated dimer consists of three singlet states and one triplet state. Neglecting overlap, the three singlet states successively possess an energy of $-2h$, 0, and $+2h$ with respect to the triplet state, in which h is the transfer integral between the dimer constituents. The spin susceptibility is easily derived from the partition function of this system in the presence of a magnetic field,

$$\chi T/C = [1 + \tfrac{1}{2}\cosh(2h/kT)]^{-1}. \qquad (6.3)$$

A value $2|h|/k = 1250$ °K (0.108 eV) gives the best reproduction of the *relative*-susceptibility behavior of LiTCNQ (from Fig. 10, curve I). Substitution of this h value in (6.3) results the susceptibility curve II of Fig. 11. The curve clearly improves upon the VB calculation of the dimer (curve I), but the deviation from the experimental behavior is still considerable (40–50% above room temperature). An adjustment of (6.3) to the experimental results needs a transfer integral with a positive temperature coefficient for its absolute value: $2|h| = 2|h^0| + 0.5kT$, which is very unlikely.

(c) In the Ising model, the exchange coupling between localized spins i and j is represented by $-2J_{ij}S_{iz}S_{jz}$. Edelstein[5] treated the problem of randomly distributed paramagnetic or diamagnetic impurities added to an antiferromagnetic Ising chain. Only nearest-neighbor exchange interactions J are considered and the paramagnetic impurity is assumed coupled to both its neighbors by a different exchange constant J', whereas the diamagnetic impurity causes a superexchange J_s between its neighbors. The quantity $\chi T/C$ depends on the reduced exchange integrals J/kT and J'/kT (or J_s/kT), as well as the impurity fraction I [Eqs. (23) and (24) in Ref. 5]. At high temperatures both expressions reduce to

$$\chi T/C - aI = e^{J/kT}, \qquad (6.4)$$

where aI is the impurity contribution. This prediction is compared with experiment in Fig. 10. The slope of the straight line at temperatures above 300 °K yields $-J/k = 1180$ °K (0.102 eV). The straightness of this line, together with the almost constant $\chi T/C$ at low temperatures (Fig. 5), imposes certain requirements upon the nature of the impurity exchange coupling. Three possibilities will be considered. (i) The impurity coupling is strongly ferromagnetic ($J'/J = -1$ or $J_s/J = -1$).

This result is rather unlikely and, moreover, it does not explain the negative deviation of the experimental curve from the straight line at temperatures below 300 °K in Fig. 10. (ii) The impurity coupling is zero ($J'=0$ or $J_s=0$). This possibility also results in constant impurity contribution to $\chi T/C$, but the objection, mentioned in (i), remains in this case. (iii) The impurity coupling is weakly antiferromagnetic. For a paramagnetic impurity we approximate

$$\chi T/C - \tfrac{3}{2}I = e^{J/kT} + IJ'/kT, \tag{6.5}$$

supposing $|J'| \leq kT < |\tfrac{1}{3}J|$.

The initial portion of the negative deviation in Fig. 10 (curve I), mentioned in (i), can be explained in this model with $J'/k \approx -17$ °K and an impurity content I of about 2.0%. However, at low temperatures ($T < 150$ °K), where the exponential part in (6.5) may be neglected, the additional temperature-dependent J' term causes a $\chi T/C$ value, which is too low, although its variation with temperature is within the experimental error. Furthermore, it should be remarked that a negative value of J' implies a decreasing χ at temperatures below $|J'|/k$. The same description holds for a diamagnetic impurity with $J_s/k \approx -23$ °K and $I \approx 6.0\%$. We can, of course, adjust the impurity content to $I \approx 2.5\%$ and fit the low-temperature value of $\chi T/C$ correctly. However, at $I = 2.5\%$, we have $J'/k = -30$ °K and this value gives the wrong temperature dependence as compared with experiment.

Hitherto, only relative susceptibilities were considered (except for the determination of I from low-temperature $\chi T/C$ values). From the high-temperature measurements we derived $J/k = -1180$ °K. Apart from its high absolute value, discussed in Sec. IV (d), this J value, substituted in (6.4), predicts a number of "free spins" $\chi T/C - aI$ (excluding impurities), which is about 45% lower than experimentally observed (Fig. 10, curves I and II). Only a linear temperature dependence $J = J^0 + 0.58kT$ is able to account for this discrepancy, but the nature of such a relationship would remain puzzling. The above discussion clearly reveals the inability of the linear Ising model to explain the susceptibility behavior of LiTCNQ in a satisfactory manner.

(d) In the theory of the alternating linear Heisenberg chain, one considers an array of tightly bound electrons that are exchange coupled to their neighbors[6,40]:

$$\mathcal{H} = \sum_{j=1}^{N/2} [-2J(1+\delta)\vec{S}_{2j} \cdot \vec{S}_{2j+1} - 2J(1-\delta)\vec{S}_{2j} \cdot \vec{S}_{2j-1} + J]. \tag{6.6}$$

An extension of exciton theory to arbitrary alternation δ and temperature has been presented by Soos.[6] The "exchange integral" J plays a dominant role in this theory. A triplet exciton band is obtained in which the band parameters are determined by the exchange interaction and alternation within a chain. At elevated temperatures, bandwidth and minimum energy separation from the singlet ground state become temperature-dependent quantities.

Starting from this theory we computed $\chi T/C$ by solving the temperature-dependent master equations, given in Ref. 6. The values $J/k = -900$ °K and $\delta = 0.10$ give the best reproduction of the absolute susceptibility behavior of LiTCNQ; this result points to a weakly alternating antiferromagnet with a low-temperature triplet-exciton bandwidth of 0.174 eV (2020 °K) and a minimum excitation energy of 0.080 eV (930 °K). However, the determination of J and δ is not exactly unique. Alternations in the range 0.00–0.20, with $-J/k = 925$–800 °K, almost fit equally well, with a slight preference for the parameters mentioned.

Although the susceptibilities, calculated with these parameters, give a good fit of the high-temperature part of the curve, the discrepancy with the experimental values at low temperatures is still considerable, as shown in curve III of Fig. 11, where predictions from the theories discussed are compared with the accurate susceptibility data for LiTCNQ. Besides this, the $|J|/k$ value of 900 °K seems improbably high in view of a calculation of the Heitler–London exchange integral J(HL) in a radical dimer, simply starting with $2p\sigma$ wave functions on both sites, separated by 3.3–3.6 Å; it yields $-J(\mathrm{HL})/k \approx 10$–$30$ °K.[41] Apart from this small direct exchange contribution, J is supposed to include important charge-transfer effects, as has been derived by Soos and Klein from their modified Hubbard model.[7] Equation (3.10) approximately reads in the case of the (1 : 1) TCNQ salts

$$J \approx -2h^2/U, \tag{6.7}$$

where h is the mean transfer integral between neighboring sites and U is the intrasite electron repulsion for doubly occupied $TCNQ^{--}$ sites, which is assumed a positive quantity by these authors. Following their arguments, insertion of the assumed J and the calculated h values for LiTCNQ in Eq. (6.7) gives $U/|h| \sim 1$. This result, however, invalidates the use of the effective spin Hamiltonian (6.6) and the Heisenberg antiferromagnet is no longer a good approximation for the alkali-TCNQ salts.

It should be pointed out that all five theories presented up to now, including the present one, are three-parameter theories. They all fit a quantity δn (the "impurity"), an "exchange" energy, and an alternation parameter (or in the dimer theories and Ising chain the temperature coefficient of ΔE, $|h|$, and J, respectively). The present theory, however, gives at least a reasonable interpretation of the parameters E_c and g via a simple SCMO cal-

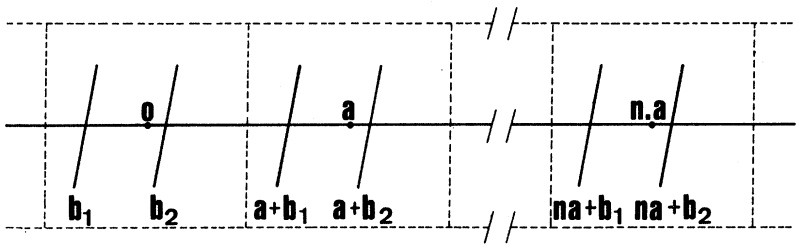

FIG. 12. Positions of the molecules relative to the center of the unit cells, labled 0, 1, ..., n, ...

culation, while it gives a very logical explanation for the variable δn, which does not have to be some impurity other than TCNQ, but just a slight stoichiometric excess or deficiency of these ions or, as discussed at the end of Sec. III, it merely arises from a small extent of disorder in the crystal. Also, the present theory easily explains the metallic behavior of the $M^+(TCNQ)_2^-$ compounds and the semiconductive behavior of the (1 : 1)-TCNQ salts. It can easily be extended to donor-acceptor (D–A) complexes and to neutral radical systems.[8] It does not, however, explain the exciton zero-field splittings observed in some TCNQ complexes. Some electron-electron interaction would have to be included to explain these excitons. As is well known, however, only a minor extension of the tight-binding theory is needed to include excitons in the model.[42]

Finally, it may be surprising that one can use simple tight-binding MO theory in a system of so little interaction. Usually, electron-electron repulsion would be sufficient to invalidate the one-electron approximation.[20] It should then again be pointed out that the low energy of the doubly occupied states in the $TCNQ^-$ chains may well justify its application to these materials.

VII. CONCLUSION

A close study of the susceptibility of Li^+TCNQ^- shows that the results are best explained by one-dimensional band theory. In this respect it appears to fall within one limit of the Hubbard theory. It is clear, that if bandwidths are small, the electron-electron interaction energies may be bigger or smaller than these bandwidths. In the case of the present compound they appear to be smaller, which, together with their linearity, makes close comparisons possible. In other TCNQ salts they may be bigger, the simple picture is destroyed and other approximations should be used. The interest in the TCNQ-ides, of course, lies particularly in this direction. It should then, however, be rembered that accurate absolute susceptibility data are required.

It might be expected that LiTCNQ would be a semiconductor with $\sigma = \sigma_0 e^{-E_g/kT}$, with E_g given by the susceptibility results. This is not the case; the activation energies for conductivity being much higher[9,12] than E_g found from susceptibility data. However, this is easily understood, when one considers the one dimensionality of the model. As shown by a number of investigators,[43] even for a one-dimensional metal one expects a gap, due to the inherent disorder of the system.

Preliminary measurements of the ac conductivity have shown a decreasing activation energy with increasing frequency, which is in accordance with expectation. It should be remembered that susceptibility measurements give the location of the one- and two-electron states, not the extent to which they are extended.

APPENDIX: BAND THEORY

In this appendix we shall calculate the electron energy bands for a periodic one-dimensional lattice with two molecules per unit cell, using the tight-binding approximation. We assume a linear chain consisting of $\frac{1}{2}N$ unit cells of length a, with periodic boundary conditions.[44] Let the molecules within the unit cell be positioned at distances b_1 and b_2 with respect to the center of the cell (Fig. 12). Then the potential may be written in the form

$$V(x) = \sum_{(n,\alpha)} U(x - a_{n,\alpha}), \tag{A1}$$

where

$$a_{n,\alpha} = na + b_\alpha . \tag{A2}$$

α (and later a similar quantity β) equals 1 or 2; na labels the center of the unit cells and $U(x)$ is the potential due to a single molecule. Further, let $\varphi(x)$ by the wave function of an electron bound to the single molecule in its ground state with energy E_0 and neglect all excited electronic states. In order to obtain a solution we assume a trial wave function of the form

$$\Psi = \sum_{(n,\alpha)} A_\alpha(n)\varphi_{n,\alpha} , \tag{A3}$$

$$\varphi_{n,\alpha} = \varphi(x - a_{n,\alpha}) \tag{A4}$$

and use the variational principle. The expectation value of the energy is

$$E = \sum_{(n,\alpha,m,\beta)} A_\alpha^*(n)A_\beta(m)H_{\alpha,\beta}(n-m) \Big/ \sum_{(n,\alpha,m,\beta)} A_\alpha^*(n)A_\beta(m)J_{\alpha,\beta}(n-m), \tag{A5}$$

where

$$J_{\alpha,\beta}(n-m)=\int \varphi^*_{n,\alpha}\varphi_{m,\beta}\,dx \tag{A6}$$

and

$$H_{\alpha,\beta}(n-m)=\int \varphi^*_{n,\alpha}[(-\hbar^2/2m)(d^2/dx^2)+V(x)]\varphi_{m,\beta}\,dx\,. \tag{A7}$$

Here we have used the fact that J and H depend only on $(n-m)$. Using (A1), one easily finds that

$$H_{\alpha,\beta}(n-m)=E_0J_{\alpha,\beta}(n-m)+\int \varphi^*_{n,\alpha}[V(x)-U(x-a_{m,\beta})]\varphi_{m,\beta}\,dx$$
$$=E_0J_{\alpha,\beta}(n-m)+h_{\alpha,\beta}(n-m)\,. \tag{A8}$$

The condition that (A5) be stationary is that

$$\sum_{(m,\beta)}[h_{\alpha,\beta}(n-m)-(E-E_0)J_{\alpha,\beta}(n-m)]A_\beta(m)=0\,. \tag{A9}$$

Due to the periodicity of the lattice, solutions of the form

$$A_\beta(m)=A_\beta e^{ipm} \tag{A10}$$

can be found. Insertion of this into (A9) shows that this is satisfied if

$$\sum_\beta[h_{\alpha,\beta}(p)-(E-E_0)J_{\alpha,\beta}(p)]A_\beta=0\,, \tag{A11}$$

where

$$h_{\alpha,\beta}(p)=\sum_n h_{\alpha,\beta}(n)\,e^{ipn} \tag{A12}$$

and

$$J_{\alpha,\beta}(p)=\sum_n J_{\alpha,\beta}(n)\,e^{ipn}\,. \tag{A13}$$

Since both $J(n)$ and $h(n)$ decrease rapidly with increasing n, because the overlap of the molecular wave functions becomes progressively smaller, it is sufficient to keep only the largest terms. Thus we approximate

$$J_{\alpha,\beta}(p)=\delta_{\alpha,\beta} \tag{A14}$$

and retain only the largest $h_{\alpha,\beta}(n)$'s, which are

$$h_{11}(0)=h_{22}(0)\equiv h_0\,,$$
$$h_{12}(0)=h_{21}(0)\equiv h_1\,, \tag{A15}$$
$$h_{21}(-1)=h_{12}(1)\equiv h_2\,.$$

Under these conditions (A11) yields the two solutions,

$$E_\pm=E_0+h_0\pm(h_1^2+h_2^2+2h_1h_2\cos p)^{1/2}\,. \tag{A16}$$

In addition, the periodicity requirement on the wave function limits p to the $\frac{1}{2}N$ values

$$p=ak\,,\quad k=4n\pi/Na\,, \tag{A17}$$

where n is any integer whose absolute magnitude is less than $\frac{1}{4}N$. Equation (A16) was also given by Adler and Brooks[45] in their paper on semiconductor-to-metal transitions.

*Supported in part by the NSF.

[1]R. G. Kepler, P. E. Bierstedt, and R. E. Merrifield, Phys. Rev. Lett. 5, 503 (1960).

[2]P. L. Nordio, Z. G. Soos, and H. M. McConnell, Ann. Rev. Phys. Chem. 17, 237 (1966), and references cited therein.

[3]D. B. Chestnut and W. D. Phillips, J. Chem. Phys. 35, 1002 (1961).

[4]J. I. Krugler, C. G. Montgomery, and H. M. McConnell, J. Chem. Phys. 41, 2421 (1964).

[5]A. S. Edelstein, J. Chem. Phys. 40, 488 (1964).

[6]Z. G. Soos, J. Chem. Phys. 43, 1121 (1965).

[7]Z. G. Soos and D. J. Klein, J. Chem. Phys. 55, 3284 (1971).

[8]P. A. Fedders and J. Kommandeur, J. Chem. Phys. 52, 2014 (1970).

[9]W. J. Siemons, P. E. Bierstedt, and R. G. Kepler, J. Chem. Phys. 39, 3523 (1963).

[10]A. Hoekstra, T. Spoelder, and A. Vos, Acta Crystallogr. B 28, 14 (1972).

[11]G. R. Anderson and C. J. Fritchie, paper presented to Society for Applied Spectroscopy, San Diego, 1963 (unpublished).

[12]J. G. Vegter, T. Hibma, and J. Kommandeur, Chem. Phys. Lett. 3, 427 (1969).

[13]J. G. Vegter, P. I. Kuindersma, and J. Kommandeur, Proceedings of the Conference on Low Mobilities, Eilat, Israel, 1971 (unpublished).

[14]D. S. Acker and W. R. Hertler, J. Am. Chem. Soc. 84, 3370 (1962).

[15]L. R. Melby, R. J. Harder, W. R. Hertler, W. Mahler, R. E. Benson, and W. E. Mochel, J. Am. Chem. Soc. 84, 3374 (1962).

[16]G. T. Pott and J. Kommandeur, Mol. Phys. 13, 373 (1967).

[17]J. van Roosmalen, J. G. Vegter, H. J. C. Berendsen, and J. Kommandeur, Rev. Sci. Instr. (to be published).

[18]M. Kinoshita and H. Akamatu, Nature (Lond.) 207, 291 (1965).

[19]Tj. Hibma (private communication).

[20]J. Hubbard, Proc. R. Soc. A 276, 238 (1963).

[21]J. G. Vegter and J. Kommandeur, Proceedings of the Fifth Molecular Crystals Symposium, Philadelphia, Pa., 1970 (unpublished).

[22]D. A. Lowitz, J. Chem. Phys. 46, 4698 (1967).

[23]H. Th. Jonkman and J. Kommandeur, Chem. Phys. Lett. 15, 496 (1972).

[24]S. Choi, J. Jortner, S. A. Rice, and R. Silbey, J. Chem. Phys. 41, 3301 (1964).

[25]J. L. de Boer and A. Vos, Acta Crystallogr. B 24, 720 (1968).

[26]K. Huang, *Statistical Mechanics* (Wiley, New York, 1963), Sec. 9.6.

[27]M. H. Cohen, Phys. Today 24, No. 5, 26 (1971), and references cited therein.

[28]C. J. Fritchie, in Acta Crystallogr. 20, 892 (1966).

[29]F. H. Herbstein, *Perspectives in Structural Chemistry*, edited by J. D. Dunitz and J. A. Ibers (Wiley, New York, 1971), Vol. 4, p. 166.

[30]R. E. Long, R. A. Sparks, and K. N. Trueblood,

Acta Crystallogr. 18, 932 (1965).
[31]Y. Iida, Bull. Chem. Soc. Jap. 42, 71 (1969).
[32]R. H. Boyd and W. D. Phillips, J. Chem. Phys. 43, 2927 (1965).
[33]B. C. Van Zorge (private communication).
[34]R. G. Kepler, J. Chem. Phys. 39, 3528 (1963).
[35]See, for instance, A. J. Dekker, *Solid State Physics* (MacMillan, London, 1963), Sec. 10.5.
[36]J. P. Farges, A. Brau, D. Vasilescu, P. Dupuis, and J. Néel, Phys. Status Solidi 37, 745 (1970).
[37]D. Bijl, H. Kainer, and A. C. Rose-Innes, J. Chem. Phys. 30, 765 (1959).
[38]D. B. Chestnut, J. Chem. Phys. 40, 405 (1964).
[39]Z. G. Soos and R. C. Hughes, J. Chem. Phys. 46, 253 (1967).
[40]Z. G. Soos, Phys. Rev. 149, 330 (1966).
[41]G. A. van der Velde and B. C. van Zorge (private communications).
[42]R. S. Knox, Solid State Phys. Suppl. 5, 1 (1963).
[43]D. Kuse and H. R. Zeller, Phys. Rev. Lett. 27, 1060 (1971); A. N. Bloch, R. Bruce Weisman, and C. M. Varma, Phys. Rev. Lett. 28, 753 (1972); H. R. Zeller, Phys. Rev. Lett. 28, 1452 (1972).
[44]See, for instance, R. E. Peierls, *Quantum Theory of Solids* (Clarendon, Oxford, England, 1964), p. 79.
[45]D. Adler and H. Brooks, Phys. Rev. 155, 839 (1967).

PHYSICAL REVIEW B VOLUME 7, NUMBER 7 1 APRIL 1973

Hyperfine-Field Measurements on Sc in Fe and Re in Ni

D. K. Gupta, A. K. Singhvi, D. N. Sanwal, and G. N. Rao
Department of Physics, Indian Institute of Technology, Kanpur, India
(Received 30 August 1972)

The hyperfine fields (H_{hf}) at ^{44}Sc nuclei in an iron matrix and at ^{187}Re nuclei in a nickel matrix are measured at room temperature using time differential perturbed (γ-γ) angular correlation technique (TDPAC). The values obtained are H_{hf} ^{44}Sc*Fe* (300 °K) = -94 ± 3 kOe and H_{hf} ^{187}Re*Ni* (300 °K) = -107 ± 3 kOe. An external magnetic field of a few kOe was applied to polarize the host matrices of iron and nickel. Using the same TDPAC technique, the magnetic moments of the 68-keV state in ^{44}Sc and of the 206-keV state in ^{187}Re are measured. The values obtained are $+(0.345 \pm 0.007)\mu_N$ and $+(5.04 \pm 0.14)\mu_N$, respectively. The measured hyperfine-field values are compared with the predictions of the existing models.

I. MAGNETIC MOMENT AND HYPERFINE-FIELD STUDIES OF ^{44}Sc

A. Introduction

Kogan *et al.*,[1] from their nuclear orientation experiments, have determined the hyperfine field H_{hf} on Sc in Fe. Measured to an order of magnitude, they reported a value of 100 kOe. The nuclear-magnetic-resonance (NMR) studies of Koi *et al.*[2] gave them a value of 58 kOe. None of these workers have measured the sign of the hyperfine field. The values reported by them vary by a factor of 2. Moreover the NMR studies often contain impurity-impurity interactions because of the poor sensitivity of the technique. Therefore, we have measured the hyperfine field using time differential perturbed (γ-γ) angular correlation technique.[3] In this technique, the concentration of the impurity atoms is so small that the impurity-impurity interactions are completely negligible. From the sense of rotation one can determine the sign of the hyperfine field. The determination of the sign of the hyperfine field on Sc in Fe is important for the studies of the systematics.[4]

The magnetic moment of the 68-keV state in ^{44}Sc was measured by Bergström *et al.*[5] and by Ristenen *et al.*[6] The values reported by them agree within the errors quoted by them. We have repeated these measurement using an external magnetic field of 7 kOe.

B. Experimental

The ^{44}Ti source was procured in solution form as chloride from NSEC (Nuclear Science and Engineering Corp., USA) and was used as such for the lifetime and the magnetic-moment studies of the 68-keV state in ^{44}Sc. For the hyperfine-field studies, the liquid source was evaporated on a thin foil of iron (99.99% pure); then the foil was melted in an argon atmosphere using an induction furnace. The molt was cooled slowly to room temperature. The resulting shining ball was rolled into a thin foil and was annealed for about 24 h at 850 °C. The annealed active foil was gradually cooled to room temperature over a period of 3 h.

Two 2×2-in. NaI(Tl) scintillators coupled to a 56-AVP photomultiplier tubes were used for the detection of the γ rays populating and depopulating the 68-keV level in ^{44}Sc. The details of the spectrometer are described elsewhere.[7] The half-life ($T_{\frac{1}{2}}$) of the 68-keV state in ^{44}Sc is measured to be 155.8 ± 2.0 nsec, which is in agreement with some of the earlier reported values[5,6] and in disagreement with some others.[8,9]